

# Land cover monitoring using coarse resolution data series

S. Le Hégarat-Masclé<sup>a,\*</sup>, C. Ottlé<sup>a</sup>, C. Guérin<sup>a</sup>

<sup>a</sup>CETP/CNRS, 10-12 av. de l'Europe, 78140 Vélizy, France – (masclé, ottle, guerin)@cetp.ipsl.fr

**Abstract** – This study focuses on the use of coarse spatial resolution (CR, pixel size about 1 km<sup>2</sup>) remote sensing data for land cover change detection and estimation. Since, in the presence of some changes, both the multitemporal class features and the pixel composition in terms of classes are unknown, the proposed algorithm is based on the iterative alternate estimation of each unknown variable: class features, and pixel composition. Final estimation of the pixel composition is constrained using a Markovian chain model, introducing the previous land cover map as a 'memory' term. This approach has been validated both using simulated data and actual data (SPOT/VGT and NOAA/AVHRR). The thematic application was the study of the evolution of an agricultural watershed during the last two decades.

**Keywords:** Change detection, land cover monitoring, coarse resolution, SPOT/VGT.

## 1 INTRODUCTION

Digital change detection deals with the quantification from multi-date imagery, of temporal phenomena, such as Aforestation-Reforestation-Deforestation, agricultural field rotation, abnormal evolution of the land surface, such as hydric stress effects on canopies, or natural disasters such as fires or floods.

In the case of high resolution data (pixel size lower than 30×30 m<sup>2</sup> such as SPOT/HRV or LANDSAT/TM), numerous change detection methods have been proposed (e.g. from Singh, 1989 to Le Hégarat-Masclé and Seltz, 2004). However, for large area processing, the survey is preferably done using coarse resolution (CR, pixel size about 1 km×1 km) sensors, such as the NOAA/AVHRR or the SPOT4/VEGETATION sensor (referred as SPOT/VGT in the following). Their spectral channels include a visible, a near infra-red and a medium infra-red band, and even some larger wavelength bands. Moreover, their high time repetition rate allows the formation of data series that can be used for the characterization of the main land cover types (bare soil surfaces, natural vegetation, crops, etc.) at regional scales (Borak *et al.*, 2000). However, for the classes whose 'objects' (fields, water areas, roads...) size is smaller than the pixel size, direct characterization is not possible. Then, to be able to use the mixed pixel measurements, the random linear model is introduced:

$$\left(\bar{X}_s\right)^t = \left(\bar{a}_s\right)^t \cdot \mathbf{y} + \left(\bar{e}_s\right)^t \quad (1)$$

-  $\bar{X}_s$  is the measurement vector attached to pixel  $s$ ,  $s \in \Omega$ , the CR image — it is of dimension  $d$ , and its component terms may correspond to different spectral signals observed at different dates included in an 'elementary' time-period  $T_i$  (change detection is performed between different  $T_i$  periods); the upperscript  $t$  denoting the transpose of vector or matrix;

-  $\bar{a}_s$  is the vector of class proportions attached to pixel  $s$  — it is of dimension  $c$ , the number of classes present in the region, and its component terms  $a_s(k)$  are the proportions of the different classes in pixel  $s$ , that satisfy:

$$\forall s \in \Omega, \begin{cases} \forall k \in [1, c] & 0 \leq a_s(k) \leq 1 \\ \sum_{k=1}^c a_s(k) = 1 \end{cases} \quad (2)$$

During  $T_i$  time period, the  $\bar{a}_s$  are assumed to be constant;

-  $\mathbf{y}$  is the matrix of dimensions  $c \times d$ , whose  $c$  lines are the transposed of the feature vectors  $\bar{y}_k$ ,  $k \in [1, c]$ , characterizing the class  $k$  during  $T_i$  ( $\bar{y}_k$  is of dimension  $d$ );

-  $\bar{e}_s$ , of dimension  $d$ , represents the errors.

Assuming that the class features are stationary within a  $N$  pixel region, the generalization of (1) to the whole region is:

$$\mathbf{X}^t = \mathbf{a}^t \cdot \mathbf{y} + \mathbf{e}^t \quad (3)$$

where  $\mathbf{X}$ ,  $\mathbf{a}$ , and  $\mathbf{e}$  are matrices of respective dimensions  $d \times N$ ,  $c \times N$ , and  $d \times N$ . From (2),  $\mathbf{a}$  is stochastic. From (3), three problems can be considered knowing  $\mathbf{X}$ :

1. Knowing the CR pixel composition  $\mathbf{a}$ ,  $\mathbf{y}$  has to be estimated. This problem is called the 'disaggregation problem'. Its main applications are surface monitoring (Faivre and Fisher, 1997) or physical model forecasting using data assimilation (Faivre *et al.*, 2000). It can be solved independently for each dimension  $j \in [1, d]$ , searching for the solution that minimizes:

$$h_1^2(j) = \sum_{s=1}^N \left[ X_s(j) - \sum_{k=1}^c a_s(k) \times y_k(j) \right]^2 \quad (4)$$

2. Knowing the class time-features  $\mathbf{y}$ ,  $\mathbf{a}$  has to be estimated. This problem corresponds to the supervised classification of a CR image. Its main application is land cover prediction using remote sensing data (Cardot *et al.*, 2003). It can be solved independently for each pixel  $s \in [1, N]$ , searching for the (2) constrained solution that minimizes:

$$h_2^2 = \sum_{j=1}^d \left[ X_s(j) - \sum_{k=1}^c a_s(k) \times y_k(j) \right]^2 \quad (5)$$

3. Neither  $\mathbf{a}$  nor  $\mathbf{y}$  is known, thus both have to be estimated. This problem corresponds to the unsupervised classification of a CR image. It is much more complex than the two former ones.

\* Corresponding author.

If we know how to solve easily the just mentioned problem 3, the problem of change detection at CR scale could be addressed simply by performing unsupervised classifications at the different periods  $T_i$  to be compared and by analyzing the classification result differences. However, besides the fact that such an approach will be rather heavy, some problems are likely to occur due to differences in the classes obtained at the different periods. In this study, we propose to address the problem of change detection at  $T_i$  using the  $T_{i-1}$  classification information, based on the same idea than the EM (Dempster *et al.*, 1977) or ICE (Pieczynski, 1992) approaches: in presence of a hidden variable in addition to the unknown one, alternate between the estimation of the hidden variable (or its distribution in classical EM) and the unknown one.

Classically, a (sub-)region where the restriction of the  $\mathbf{a}$  matrix is known is used to estimate the class feature matrix  $\mathbf{y}$  from the Problem 1 (among the three problems mentioned just before) solution. Then, assuming it is stationary,  $\mathbf{y}$  is used to estimate the restriction of the  $\mathbf{a}$  matrix to the regions where it is unknown. In this study, we relax the assumption of the *a priori* knowledge of a (sub-)region  $\mathbf{w}$  where  $\mathbf{a}$  is known. Therefore, the first step is now to determine automatically the two subsets of pixels candidate to be unchanged,  $\mathbf{w}$ , and of pixels candidate to be changed,  $\Omega-\mathbf{w}$ . This step provides the 'change detection first guess' and its result,  $\mathbf{w}$ , is used to estimate  $\mathbf{y}$ . The second step aims at providing a new estimation of the class repartition within CR pixels. It is compared to the previous repartition to derive the 'change detection *a posteriori* estimation'. To be successful, the use of this approach must be restricted to the case where the changes are minority. Section II details the proposed approach and its two steps: change detection, and change estimation. Section III first validates the method in the case of simulated data. Then, the results obtained using SPOT/VGT and NOAA/AVHRR actual data to monitor the land cover over the Val de Saône watershed (France) are presented. Section IV gathers our conclusions.

## 2 CHANGE DETECTION AND ESTIMATION

Here, it is assumed that image preprocessing, and in particular coregistration, is done correctly (the difficulties of misregistration modeling make impractical any other assumption).

The relative normalization of the  $d$  components of  $\bar{X}_s$  is also considered as a preprocessing step. Indeed, the use of Euclidian norm throughout the entire study implicitly assumes an equal noise power (or variance) for the  $d$  dimensions.

### 2.1 Determination of a subset of pixels without change, and class feature learning

The problem considered here is similar to Problem 1, except that we do not know on which sub-part of the image, or pixel subset  $\mathbf{w}$ , our prior knowledge of land cover is valid. In other words, defining the equation system (3) from all the CR image pixels, some equations are erroneous due to the occurred changes in some CR pixels  $s$ , that make prior  $\bar{\mathbf{a}}_s$  values invalid. Such equations have to be removed from (3). The proposed method estimates simultaneously the pixel subset  $\mathbf{w}$ , i.e. the set of the pixels candidate to present no change in their composition ( $\bar{\mathbf{a}}_s$  values), and the class features. The label changed or unchanged (i.e. belonging to  $\mathbf{w}$  or to  $\Omega-\mathbf{w}$ ) is the hidden field, and the class features  $\mathbf{y}$  are the unknown variables. According to the mean

square error minimization criterion,  $\mathbf{y}$  is estimated from the restriction of (3) to  $\mathbf{w}$  as:

$$\forall j \in [1, d] \quad [\tilde{\mathbf{y}}]_j = \underset{[\mathbf{y}]_j}{\operatorname{argmin}} \left( \sum_{s \in \mathbf{w}} \left[ X_s(j) - \sum_{k=1}^c \mathbf{a}_s(k) y_k(j) \right]^2 \right) \quad (6)$$

For  $\mathbf{w}$  estimation, we consider a threshold on the pixel composition difference between initial value and new estimation. It can be shown that such it is much more robust than the more intuitive threshold on the quadratic error (Le Hégarat-Masclé *et al.*, 2005).  $\mathbf{y}$  and  $\mathbf{w}$  are derived simultaneously using an iterative alternate estimation. Two steps are carried on at each iteration: (i)  $\mathbf{y}$  estimation from the knowledge of the restriction of  $\mathbf{a}$  to  $\mathbf{w}$  from (6), (ii)  $\mathbf{w}$  pixel composition re-estimation knowing  $\mathbf{y}$  from:

$$\forall s \in \mathbf{w}, \quad \tilde{\mathbf{a}}_s = \underset{\bar{\mathbf{a}}_s}{\operatorname{argmin}} \left( \sum_{j=1}^d \left[ X_s(j) - \sum_{k=1}^c \mathbf{a}_s(k) y_k(j) \right]^2 \right) \quad (7)$$

(7) minimization is both subject to bounds on the variables and linearly constrained. Optimization is based on a two-phase quadratic programming method (Gill *et al.*, 1984). Before re-iteration,  $\mathbf{w}$  is updated by removing the pixels exhibiting a  $\Delta \mathbf{a}$  value greater than the current threshold (in our case empirically decreasing geometrically from 0.5 to 0.05).

At the end of this algorithm step, two issues have been derived: an estimate of  $\mathbf{y}$ , and a subset of CR pixels associated with changes:  $\mathbf{w}_{ch} = \Omega - \mathbf{w}$ . Assuming that all changes are land cover changes, a new estimate of  $\mathbf{a}$  for all these pixels can be attempted.

### 2.2 Re-estimation of the composition of the pixels not included in the previous subset, and specification of the changes

The problem considered here is similar to Problem 2 described in the Introduction. We assume that, from the previous step, all the CR pixels with changes are included in  $\mathbf{w}_{ch}$ . In fact,  $\mathbf{w}_{ch}$  is likely to contain also unchanged composition pixels, but exhibiting a high noise level. The resolution of (7) leads to mathematically optimal solutions – in terms of quadratic error, without considering the 'physical' meaning of the solutions. Now, in some cases, the secondary minima may be more realistic for the physical application. Therefore, we propose that the solution also be as close as possible to the initial land cover map. It is justified since:

- first, some CR pixels are re-estimated even though they have not changed ( $\mathbf{w}_{ch}$  contains also unchanged pixels exhibiting a high noise level);
- secondly, in the case of the CR pixels presenting some actual changes, for a given pixel, the changes are likely to concern a limited number of classes (and then  $\mathbf{a}_s(k)$  terms), e.g. the redeployment of grassland to crops impacts only two classes.

Mathematically, the new function to minimize is:

$$\mathbf{h}_3^2 = \left\| \mathbf{y}^t \cdot \bar{\mathbf{a}}_s - \bar{X}_s \right\|^2 + \mathbf{g} \left\| \bar{\mathbf{a}}_s - \bar{\mathbf{a}}_s^{(0)} \right\|^2 \quad (8)$$

where, in addition to previous notation definition,  $\bar{\mathbf{a}}_s^{(0)}$  is the prior value of  $\bar{\mathbf{a}}_s$ , and  $\mathbf{g}$  is a weighting parameter,  $\mathbf{g} \in \mathfrak{R}^+$ . It monitors

the relative importance of the 'reminder' or 'memory' term: For  $\mathbf{g}=0$ , the minimization is performed only considering the 'data attachment' term  $\left\| \mathbf{y}^t \cdot \bar{\mathbf{a}}_s - \bar{\mathbf{X}}_s \right\|^2$ , conversely to the  $\mathbf{g} = +\infty$  case where the obtained solution is the previous composition map independently of the 'data attachment' term. In our case,  $\mathbf{g}$  is determined empirically, and the fact that the best results are obtained for a non-null value of  $\mathbf{g}$  will state (section III) the relevance of the proposed 'reminder' or 'memory' term. For computational aspects, we note that (8) can also be written:

$$\mathbf{h}_3^2 = \left\| \begin{pmatrix} \mathbf{y}^t \\ \mathbf{g} \mathbf{I}_c \end{pmatrix} \bar{\mathbf{a}}_s - \begin{pmatrix} \bar{\mathbf{X}}_s \\ \mathbf{g} \bar{\mathbf{a}}_s^{(0)} \end{pmatrix} \right\|^2 \quad (9)$$

where  $\mathbf{I}_c$  is the identity matrix of dimension  $c$ , and the newly involved vector and matrix are obtained by line concatenation operation of previously defined vectors and matrices. The minimization is achieved using the same procedure as for (7).

### 3 RESULTS

#### 3.1 Case of simulated images

To validate our approach in a case where all parameters are known, we consider simulated data. Eight classes have been simulated, whose temporal signal features correspond to different land types: water, bare soil, vegetation (forest, grassland, crops). Some changes have occurred in the initial land cover map. According to the new label map and the class features, high resolution (HR) data have been simulated under the assumption of white noise and Gaussian laws representing the class conditional probabilities. CR data are obtained by simple average of the values of the  $50 \times 50$  HR pixels included in each CR pixel.

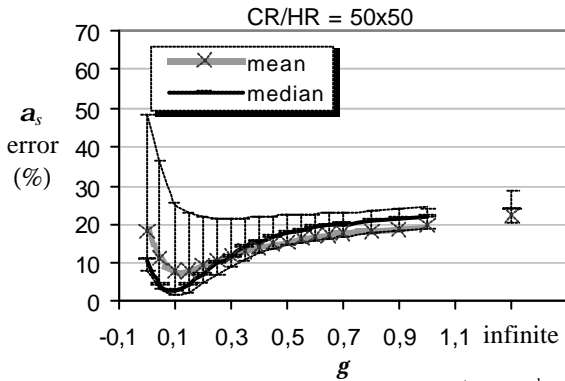


Figure 1.  $\Delta \mathbf{a}_s$  global statistics (mean, median, 1<sup>st</sup> and 3<sup>rd</sup> quartiles) estimated over  $\mathbf{w}_{ch}$ , for the resolution ratio  $50 \times 50$ .

The  $\mathbf{y}$  matrix is estimated using the proposed algorithm. Convergence is achieved for 5 iterations. The error on class feature estimation remains less than 0.1 for class feature values ranging from 0 to 1. Fig. 1 shows the  $\mathbf{a}_s$  error statistics: mean, median, and 1<sup>st</sup> and 3<sup>rd</sup> quartiles estimated over the set  $\mathbf{w}_{ch}$ , versus the parameter  $\mathbf{g}$ . Restriction to  $\mathbf{w}_{ch}$  allows to focus on the detected changes and the pixel composition re-estimation. The value at the abscissa labelled 'infinite' corresponds to the case where no change detection was performed. Fig. 1 states the interest of the 'reminder' or 'memory' term ( $\mathbf{g} \neq 0$ ). In the absence of this term, the composition error mean value is almost equal to 18% (median

value almost 11%). Best result is then obtained for  $\mathbf{g} = 0.1$ : composition error mean value lower than 8% (median value lower than 3%). Looking at the distributions of the  $\mathbf{a}$  errors versus the CR pixel change rate, obtained in different cases of  $\mathbf{g}$  value, we can check that the highest are the change rate values, the lowest should be  $\mathbf{g}$ . In our case,  $\mathbf{g} \neq 0$  improves the results until change rate values around 30% are reached.

#### 3.2 Land use monitoring in an agricultural watershed

The data under consideration in this section were acquired over the Val de Saône (France) which is the downstream region of the Saône watershed. Over this region a database gathering coarse resolution images from two satellite sensors are available. First data series have been acquired by the NOAA/AVHRR (Advanced Very High Resolution Radiometer) sensor. The considered daily data are geo-referenced in Lambert II with pixel size equal to  $1 \text{ km} \times 1 \text{ km}$ . Among the available channels, the Red, the NIR, and the MIR Top Of Atmosphere reflectances were selected. Two other data series have been acquired by the VGT sensor: S10 series and P series (only produced by the VITO center, <http://www.vgt.vito.be>). The P series contains daily data corresponding to the 'Physical' measurements (reflectance values). The S10 product is a mosaic image corresponding to the highest radiometric value measured within ten days (three 10-day period per month) for each pixel. The VGT sensor has four spectral channels: the Blue, the Red, the NIR, and the MIR. For VGT series, the projection is Lambert Northern Europe, with a pixel size equal to  $1 \times 1 \text{ km}^2$ . For each series, the considered images have been selected according to a clear sky criterion, and an angle constraint criterion in the case of the S10 series. For the VGT-P series, the available clear sky images were sufficiently numerous in 2000. In the case of the other series, data acquisitions taken in 1999 or 2001 were added to data in 2000. Besides the considered reflectance channels measured by each sensor, vegetation indices, such as the GEMI (Global Environment Vegetation Index, Pinty et Verstraete, 1992, chosen as *a priori* little dependent on atmospheric effects), have been derived. Indeed, they are very useful to distinguish land cover types in an agricultural area, just as the cover fraction that was also computed using the empirical relationships proposed in (Weiss *et al.*, 2002).

To update the Corine Land Cover map established in the 1980's, the proposed methodology has been applied to each data series, and the results were projected in the same Lambert II coordinate system for comparison. The results are consistent. In particular, those obtained using the NOAA/AVHRR data are very close to those obtained with the SPOT/VGT-S10 series. Tab. A gives the linear fitting parameters between the different estimations of pixel composition (in terms of land cover proportions) obtained from each data series, e.g. the linear relationship between the urban class estimated proportion in AVHRR pixel is  $-0.00$  plus  $1.03$  times the urban class estimated proportion in VGT-S10 pixel, with a correlation coefficient equal to 0.98. For this couple of data series, the linear fitting is very close to unity (slope values ranging from 0.94 to 1.07 and offset absolute values lower than 0.04), with correlation coefficients ranging from 0.91 to 0.98. A part of the observed noise is due to the re-projection, which does not take into account the class location within CR pixels. Fig. 2 shows the VGT-AVHRR pixel proportion estimate versus the VGT-S10 one, for the two main land cover types on the watershed: forest and crop fields (respectively  $\approx 12\%$  and  $58\%$  in Corine Land Cover 1980's map). For the other CR result couples, similar results have

been obtained: Tab. A gives the linear relationships class by class.

class	AVHRR vs VGT-S10		AVHRR vs VGT-P		VGT-S10 vs VGT-P	
	Y=	r	Y=	r	Y=	r
urban	-0.00+1.03.X	0.98	-0.02+1.03.X	0.89	-0.02+1.01.X	0.91
forest	0.00+1.04.X	0.97	-0.00+1.03.X	0.91	-0.00+0.99.X	0.94
water	0.00+1.07.X	0.92	0.00+0.94.X	0.72	-0.00+0.78.X	0.70
crop	-0.01+0.95.X	0.91	0.03+0.98.X	0.86	0.07+0.97.X	0.89
grassland	0.04+0.94.X	0.91	0.02+0.91.X	0.87	-0.00+0.91.X	0.90
vineyard	-0.00+1.02.X	0.98	-0.00+1.00.X	0.95	-0.00+0.98.X	0.97

Table A. For each land cover type, linear regression and correlation coefficient between a couple of estimations of the CR pixel proportion derived from NOAA/AVHRR, SPOT/VGT-S10, or SPOT/VGT-P.

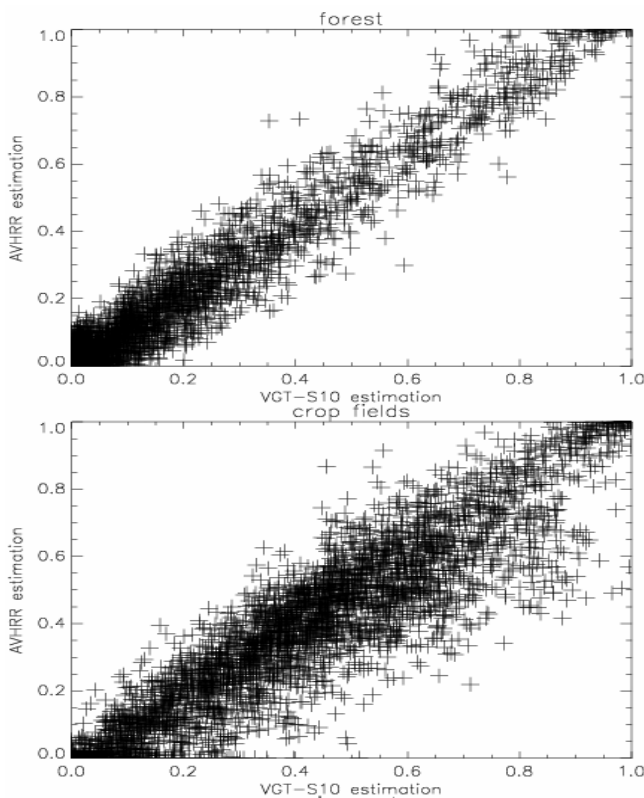


Figure 2. Val de Saône results: AVHRR pixel proportion estimates versus VGT-S10 ones, for forest and crop areas.

From the thematic point of view, the main results are the following: urban areas: increase of some cities already existing; forest: slight decrease of the small forested areas still present in 1980's in the agricultural part of the watershed; water: increase of the number of aquaculture ponds, and decrease of the Saône river extent in the Northern part of the watershed; crop fields: important increase (about 11.3% at watershed scale); grassland: important decrease (replaced by crop fields) except at the borders of the river; vineyards: no noticeable change. These changes are consistent with the *a priori* knowledge of the watershed. The detection of these changes have then to be exploited in some future studies on the impact of the land cover change on the meteorological processes or hydrological ones.

## 4 CONCLUSIONS

This paper presents a methodology for change detection using coarse spatial resolution (CR) time series. It relies on a linear mixing model for the CR pixels. The input data are: the CR series, the number of classes, and the previous CR pixel composition. In terms of change importance, the application domain of the method is restricted to minor changes. Besides, from actual results, due to the noise in CR pixel re-estimation, the method is not efficient for too few changes. Several explanations can be given for the presence of this 're-estimation' noise, such as the sensor acquisition geometry (even if for the comparison a common reference system was used). Future studies will deal with the use of medium resolution sensors ( $\approx 250 \times 250 \text{ m}^2$ ), such as MERIS/Envisat or MODIS/Terra. The decrease of the pixel size may induce a decrease of the minimum change value detected.

## 5 REFERENCES

- J. Borak, E. Lambin, A. Strahler, "The use of temporal metrics for land cover change detection at coarse spatial scales", *Int. J. of Rem. Sens.*, **21**(6-7):1415-1432, 2000.
- H. Cardot, R. Faivre, M. Goulard, "Functional approaches for predicting land use with the temporal evolution of coarse resolution remote sensing data", *J. of Applied Stat.*, **30**:1185-1199, 2003.
- A. Dempster, N. Laird, and D. Rubin, "Maximum likelihood from incomplete data via the EM algorithm" *J. of the Royal Stat. Soc., Series B*, **39**(1):1-38, 1977.
- R. Faivre, and A. Fischer, "Predicting crop reflectances using satellite data observing mixed pixels", *J. of Agr. Bio. and Env. Stat.*, **2**:87-107, 1997.
- R. Faivre, C. Bastié, and A. Husson, "Integration of VEGETATION and HRVIR data into yield estimation approach", *proc. of Vegetation 2000*, Ispra, Varese (Italy), pp.235-240, 2000.
- P. Gill, W. Murray, M. Saunders, and M. Wright, "Procedures for optimization problems with a mixture of bounds and general linear constraints", *ACM Trans. on Math. Software*, **10**:282-298, 1984.
- S. Le Hégarat-Masclé, and R. Seltz, "Automatic change detection by evidential fusion of change indices", *Rem. Sens. of Env.*, **91**(3-4):390-404, 2004.
- S. Le Hégarat-Masclé, C. Ottlé, and C. Guérin, "Land cover change detection at coarse spatial scales based on iterative estimation and previous state information", *Rem. Sens. of Env.*, to appear, 2005.
- W. Pieczynski, "Statistical image segmentation", *Mach. Graphics Vision*, **1**(1/2):261-268, 1992.
- B. Pinty, and M. Verstraete, "GEMI: A non linear index to monitor global vegetation from satellite", *Vegetation*, **101**:15-20, 1992.
- A. Singh, "Digital change detection techniques using remotely-sensed data", *Int. J. of Rem. Sens.*, **10**(6):989-1003, 1989.
- M. Weiss, F. Baret, M. Leroy, O. Hautecoeur, C. Bacour, L. Prévot, N. Bruguier, "Validation of neural net techniques to estimate canopy biophysical variables from remote sensing data", *Agronomy: Agricult. and Env.*, **22**:547-553, 2002.

## Acknowledgements

This work was partly supported by the French INSUE (*Institut National des Sciences de l'Univers et de l'Environnement*). The Corine land cover database was provided through the Gewex-Rhone program by the French Institute of the Environment. SPOT data have been obtained by the ISIS French program of the CNES.